2. Experimental

2.1. Catalyst preparation

All materials with analytical purity were purchased from Merck and used without further purification. The Ba-Sr/ZSM-5 catalyst was prepared using the incipient wetness impregnation method. At first ZSM-5 zeolite was calcined at 600°C for 6 h. The calcined ZSM-5 zeolite was impregnated with aqueous solutions of $Sr(NO_3)_2$ to generate 6 wt.% Sr/ZSM-5 catalyst (A). Then, for preparation the catalyst containing 4 wt.% Ba, the solution of $Ba(NO_3)_2$ was impregnated to (A). The 10 wt.% Ba-Sr/ZSM-5 (Sr/Ba=3/2) catalyst was dried at 120°C for 12 h after each impregnation step. Finally, the dried catalyst was calcined at 600°C for 6 h with a heating rate of 3°C/min to produce heterogeneous solid catalyst.

2.2. Catalyst characterization

2.2.1. X-Ray diffraction (XRD)

The crystal structures of the synthesized nanocatalysts were recorded with a Philips X' Pert (an accelerating voltage of 40 kV, and an emission current of 30 mA) X-ray diffractometer, using a Cu-Kα radiation source (λ=1.542 Å) which combined with the nickel filter in the 2θ range of 0°-120°.

2.2.2. Fourier transform infrared (FT-IR) spectrometry

Fourier Transform Infrared spectroscopy (ALPHA, Bruker, Germany) was used to provide information about the structure of the catalyst material, and the sample was scanned in the range of 400 to 4000 1/cm.

2.2.3. Scanning electron microscopy (SEM)

Scanning Electron Microscopy (SEM) was used to determine the morphology and particle size of the catalyst crystals using an S-360 Oxford Eng scanning electron microscopy.

2.2.4. N_2 physisorption measurements

The specific surface area, total pore volume and the pore diameter were measured using a N_2 adsorption-desorption isotherm at liquid nitrogen temperature (-196°C), using a NOVA 2200 instrument (Quantachrome, USA). Prior to the adsorption-desorption measurements, all the samples were degassed at 110°C in a N_2 flow for 2 h to remove the moisture and other adsorbates.

2.2.5. Transmission electron microscopy

TEM investigations were done by using a Hitachi H-7500 (120kV). The sample for TEM study was prepared by ultrasonic dispersion of the catalyst in ethanol.

2.3. Catalyst testing

The yield and compositions of the methyl ester products were determined using GC-Mass (GC Agilent 6890N model and Mass Agilent 5973N model) equipped with a flame ionized detector (FID). A capillary column (HP-5) with Column length (60 m), Inner Diameter (0.25 mm) and 0.25 µm film thickness was used with helium as the carrier gas. The temperature program for the biodiesel samples started at 50°C and ramped to 150°C at 10˚C/min. The temperature was held at 150°C for 15 min and ramped to 280°C at 5°C/min. The holding time at the final temperature (250°C) was 5 min. Also, the injector was used from kind split/splitless.

2.4. Kinetic study

To determine the kinetics of the transesterification reaction, the effect of reaction temperature and reaction time were investigated. All reactions were carried out in a 250 ml glass reactor equipped with a condenser. The catalyst was dispersed in the 9:1 methanol to oil molar ratio with magnetic stirring of 500 rpm. Then, the sunflower oil with the average molecular weight of 863.3 g/mol calculated from the saponification value (S.V= 194.9 mg KOH/g) was added, and the mixture was heated at reflux to selected reaction temperatures and times. The reaction temperature was varied from 323-333 K and reaction time was varied from 0 to 180 min. After the reaction completion, two layers formed. The upper layer (light phase) contained biodiesel and methanol, whereas the bottom layer (heavy phase) contained glycerol. Centrifugation was carried out to separate catalyst, and the excess amount of methanol was evaporated. At last, the biodiesel and glycerol were separated under gravity using a decanter. The obtained biodiesel was washed 3 times with warm water and the samples concentration calculated according to mole fraction at mentioned time [23,32]. The 10 wt.% Ba-Sr/ZSM-5 (Sr/Ba=3/2) catalyst showed high catalytic activity for biodiesel production and the biodiesel yield reached 86.69% at 333 K.

2.5. Analysis of kinetics models

The general equation of transesterification of triglycerides can be presented by the following stoichiometric Eq. 1:

$$A + 3B \overset{\text{Catalyst}}{\longleftrightarrow} 3R + S \qquad (1)$$

Where A, B, R and S are triglyceride (TG), methanol, methyl ester (ME) and glycerol, respectively. This reaction consists of three step reactions to convert TG to biodiesel and glycerol. In the first step, the triglyceride was reacted with one molecule of methanol and produced diglyceride (DG) and one molecule of methyl ester.

Then, the molecule of DG reacted with another molecule of methanol to produced monoglyceride (MG) and one molecule of methyl ester. Finally, the reaction between MG and methanol produce ME and glycerol.

Based on previously reported mechanistic considerations, it was assumed that the reaction is a single step transesterification, and the intermediate reactions of DG and MG have been ignored [18,19, 33-38]. So, the rate law of transesterification reaction can be expressed by Eq 2:

$$-r_a = -\frac{d[A]}{dt} = k'.[A].[B]^3 \quad (2)$$

Where, k' is the equilibrium rate constant. According to the Eq 2, this overall conversion should follow a forth order reaction rate law [38]. However, according to our results and other works published [19,39-45] pseudo-first and pseudo-second order reactions for the transesterification process of sunflower oil have been proposed.

2.5.1. Pseudo-first order kinetics model

For the pseudo-first order mechanism, the following assumptions were proposed:

1- The conversion of TG follows as the pseudo-first order transesterification reaction kinetics.
2- The reverse reaction could be ignored, and change in catalyst concentration during the reaction can be assumed to be negligible due to using of sufficient amount of catalyst with respect to sunflower oil to shift the reaction equilibrium to the forward reaction.
3- The concentration of methanol was considered to be constant due to the excess amount of methanol.

So, the pseudo-first order rate law can be expressed as:

$$-r_a = -\frac{d[A]}{dt} = k.[A] \quad (3)$$

Where k is the modified rate constant,

$$k = k'.[B]^3 \quad (4)$$

By the integration of Eq. 3:

$$\ln[A_0] - \ln[A] = k.t \quad (5)$$

Based on the mass balance,

$$X_R = 1 - \frac{[A]}{[A_0]} \quad (6)$$

Where X_R is the conversion of methyl ester,

$$[A] = [A_0](1 - X_R) \quad (7)$$

Also,

$$\frac{dX_R}{dt} = k(1 - X_R) \quad (8)$$

Finally,

$$-\ln(1 - X_R) = k.t \quad (9)$$

Fig. 1 shows the plot of $-\ln(1 - X_R)$ versus reaction time according to pseudo-first order kinetics model.

2.5.2. Pseudo-second order kinetics model

For the pseudo-second order mechanism, the following assumptions were proposed:

1- The overall reaction follows a second order reaction rate law, and due to the high molar ratio of methanol to sunflower oil in methanol phase, the rate of transesterification reaction could be expressed as a function of TG concentration only.
2- The reverse reaction could be ignored due to the excess of methanol and low concentration of product. So, the methanolysis of TG is the irreversible pseudo-second order reaction in the early period of the transesterification reaction.
3- The reaction mixture of two liquid phases (oil and methanol) is perfectly mixed, so the uniform composition could be assumed.

If the pseudo-second order transesterification reaction was assumed, the reaction rate can be expressed as:

$$-r_a = -\frac{d[A]}{dt} = k_2.[A]^2 \quad (10)$$

Where k_2 is reaction rate constant for the irreversible pseudo-second order.

$$[A] = [A_0](1 - X_R) \quad (11)$$

That is,

$$-\frac{dX_R}{dt} = k_2.[A_0].(1 - X_R)^2 \quad (12)$$

Integration of Eq. 12 yields:

$$\frac{1}{1-X_R} = k_2.[A_0].t \quad (13)$$

Fig. 2 shows the plot of $\frac{1}{1-X_R}$ versus reaction time according to pseudo-second order kinetics model.

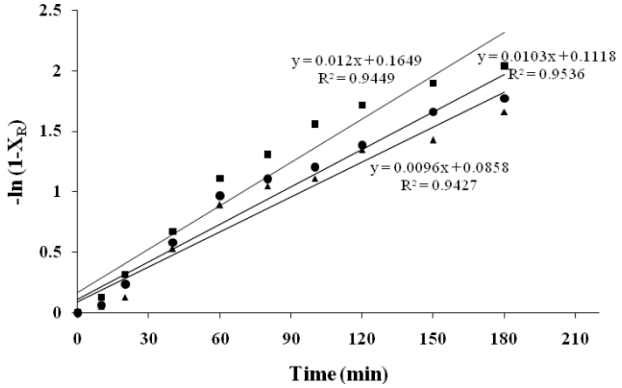

Fig. 1. Plots of –ln ($1-X_R$) versus time during transesterification reaction of sunflower oil at 323 K -▲; 328 K-● and 333 K-■.

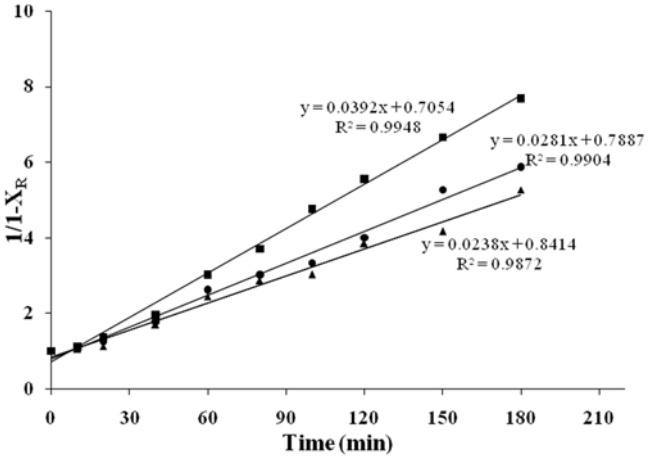

Fig. 2. Plots of $1/1\text{-}X_R$ versus time during transesterification reaction of sunflower oil at 323 K -▲; 328 K-● and 333 K-■.

Based on these two kinetics models and the experimental data, the concentrations of ME at different times according to the moles fraction and the rate constants at each temperature were calculated. Also, the pre-exponential coefficient and activation energy were calculated by plotting the logarithm of the rate constants (ln *k*) versus *1/T* of absolute temperature using the Arrhenius equation.

3. Results and Discussion

3.1. Characterization of the catalyst

The XRD pattern of the 10wt.% Ba-Sr/ZSM-5 (Sr/Ba=3/2) catalyst which calcined at 600 ºC for 6 h is shown in Fig. 3. The actual oxide phases, $Al_2Si_2O_8$, BaO, SrO (monoclinic) and $Al_2O_3SiO_2$ (orthorhombic) were clearly identified by XRD. It is clear that the catalyst particle size which calculated by Scherrer equation was in nano dimension (51.8 nm) [46].

The FTIR spectrum of the 10wt.% Ba-Sr/ZSM-5 (Sr/Ba=3/2) catalyst which calcined at 600 ºC for 6 h is shown in Fig. 4. The broad band at 3454 cm^{-1} and 1636 cm^{-1} is ascribed to the stretching and bending vibration of the OH of groups water in catalyst, respectively. The bands of hydroxyl groups of ZSM-5 zeolite are divided to terminal silanols (3740 cm^{-1}), outside the crystal lattice OH (3680cm^{-1}) and hydroxyl groups at defect sites (3720 cm^{-1}) and the bridge OH as Al-Si-OH with the character Brønsted acid sites (3600-3650 cm^{-1}). The Lewis acid sites can be found in the region of 1490cm^{-1} and, the Brønsted acid sites in the 1540-1630 cm^{-1} region [26]. The band at 844cm^{-1} is ascribed to the Al-O-Al stretching mode while the band in the range of 520-600 cm^{-1} is related to SrO and BaO and the bending modes of Al_2O_3 [47]. Also, the band in the region of 440 cm^{-1} can be assigned to Si-O-Si bending modes [48]. The SEM micrographs of precursor and calcined Ba-Sr/ZSM-5 catalyst are shown in Fig. 5. As indicated particles size of precursor is between 72 and 120 nm, and several large particles agglomerations are observed (Fig. 5a). Also, before calcination catalyst precursor has less homogeneous morphology. Calcination process at 600˚C for 6 h by heating rate of 3˚C/min slightly modified the morphology of the catalyst particles, and led to reduce particles agglomeration (Fig. 5b). The BET surface areas, pore volume and pore diameter (using BJH adsorption isotherm) [49], of the precursor and calcined Ba-Sr/ZSM-5 catalyst displayed in Table 1. It can be seen that the Ba-Sr/ZSM-5 catalyst which calcined at 600 ºC for 6 h exhibited a high surface area value of 224.3 m^2/g. As it mentioned, this catalyst showed a high catalytic activity due to its high BET surface area. Moreover, the precursor exhibited a lower surface area value of 156.3 m^2/g.

The Ba-Sr/ZSM-5 catalyst was characterized with TEM (Fig. 6). As shown in Fig. 6, the particle sizes are from 40–45 nm. This result confirms obtained results that was studied by using the Scherrer equation.

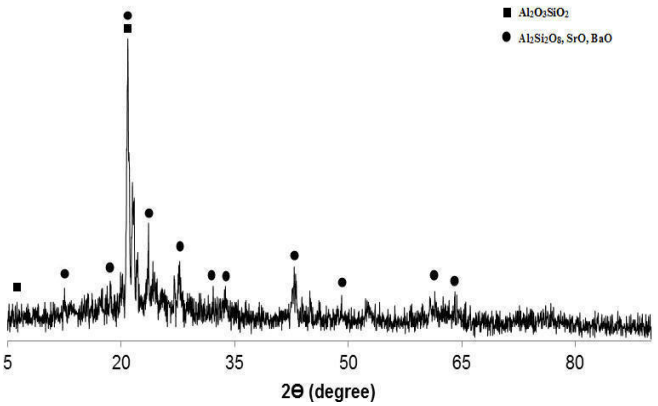

Fig. 3. X-ray diffraction pattern of Ba-Sr/ZSM-5 catalyst was calcined at 600 °C for 6 h.

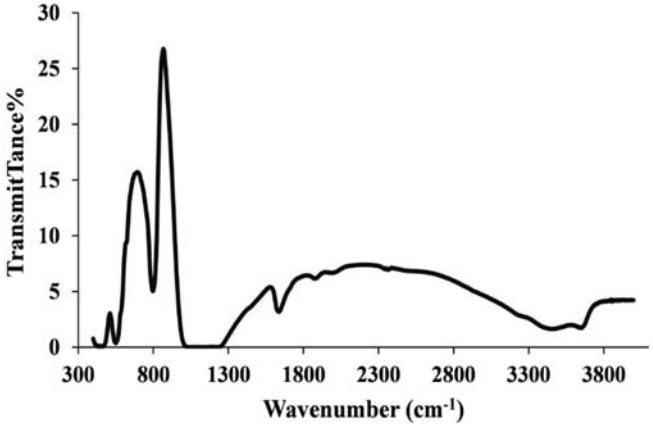

Fig. 4. FTIR spectrum of Ba-Sr/ZSM-5 catalyst was calcined at 600°C for 6 h.

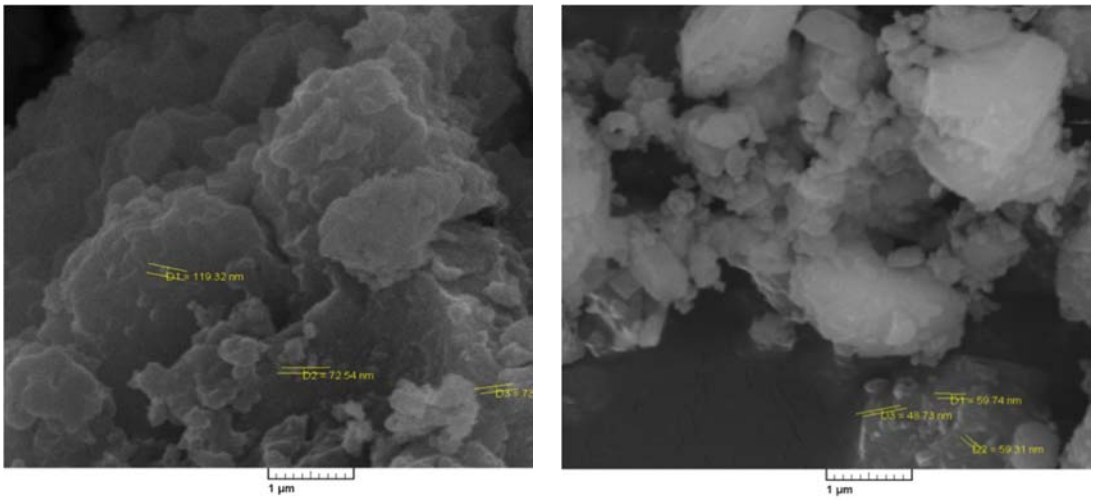

(a) **(b)**

Fig. 5. The SEM images of Ba-Sr/ZSM-5catalyst; (a) precursor and (b) calcined catalyst at 600°C for 6 h.

Table 1. N_2 adsorption-desorption measurements of precursor and calcined Ba-Sr/ZSM-5 catalyst prepared at 600°C for 6 h.

Parameter	Precursor	Calcined catalyst
S.S.A (m^2/g)	153.2	224.3
P.V (cm^3/g)	0.62	0.79
P.D (Å)	17.53	18.54

S.S.A: specific surface area
P.D: pore diameter
P.V: pore volume

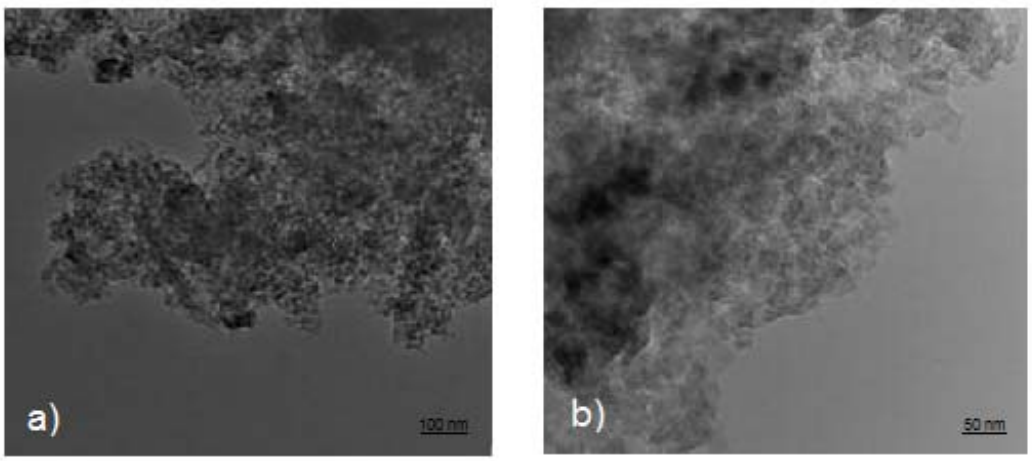

Fig. 6. The TEM image of Ba-Sr/ZSM-5catalyst; (a) precursor and (b) calcined catalyst at 600°C for 6 h.

3.2. Pseudo-second order reaction approximation

The present kinetic study assumes an irreversible reaction mechanism of pseudo-first and pseudo-second order for biodiesel production from sunflower oil and methanol in the presence of 10wt.% Ba-Sr/ZSM-5 (Sr/Ba=3/2) catalyst. Fig. 1 and Fig. 2 show the pseudo-first order and pseudo-second order, kinetics diagrams, respectively. According to the regression coefficient (R^2), there is an excellent fit to the pseudo-second order kinetics model. So, rate constant, activation energy, pre-exponential coefficient calculated based on pseudo-second order kinetics model for this reaction.

3.3. Rate constant, activation energy and pre-exponential coefficient

As shown in Fig. 2, the transesterification of sunflower oil reaction rate constants can be estimated from the slope of $\frac{1}{1\text{-}X_R}$ versus time plots. Moreover, the mathematical relation between rate constants and temperature can be expressed by the following Arrhenius equation:

$$k = A.\exp(\frac{-E_a}{RT}) \quad (14)$$

From integration of Eq. 14:

$$lnk = lnA - \frac{E_a}{RT} \quad (15)$$

Where k, A, E_a, R and T are the rate constant (min^{-1}), the pre-exponential coefficient (min^{-1}), the activation energy ($kJ.mol^{-1}$), the universal gas constant (8.314 $J.mol^{-1}.K^{-1}$) and the absolute temperature (K), respectively. As shown in Fig. 7, the plot of ln k versus *1/T* gives a straight line with intercept and slope of ln A and $-E_a/R$, respectively. The activation energy and the pre-exponential coefficient of sunflower oil transesterification reaction using the Arrhenius equation were 67.03 kJ/mol and 9.29×10^8 1/min, respectively. So, according to pseudo-second order kinetics model and experimental data, the rate constants follow the Arrhenius equation.

4. Conclusions

The Ba-Sr/ZSM-5 nanocatalyst prepared by incipient wetness impregnation method followed by calcination at 600°C for 6 h with a heating rate of 3°C/min and showed high catalytic activity for biodiesel production. The transesterification reactions of sunflower oil using this catalyst were carried out at reflux of methanol with methanol to oil molar ratio of 9/1 and reaction time in the range of 0-180 min with mechanical stirring of 500 rpm. An irreversible pseudo-second-order kinetics that considers only the kinetics of triglyceride conversion were obtained in the best modeling of experimental data, at reaction temperatures in the range of 323-333 K. The activation energy and the pre-exponential coefficient of sunflower oil transesterification reaction using the Arrhenius equation were 67.03 kJ/mol and 9.29×10^8 1/min, respectively.

Acknowledgements

We are grateful to the Iran Nanotechnology Initiative Council (INIC) for their partial support on this project.

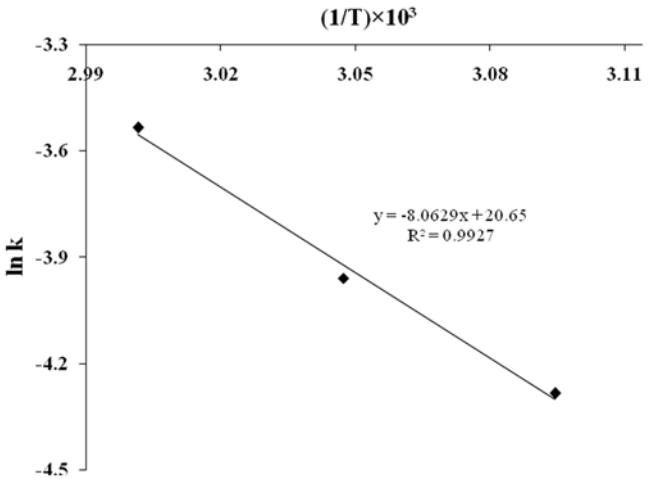

Fig. 7. Arrhenius plot of ln k versuss *1/T* for transesterification reaction of sunflower oil.

References

[1] D. Kumar, A. Ali, Biomass Bioenerg. 46 (2012) 459-468.
[2] P. Patil, V.G. Gude, S. Pinappu, S. Deng, Chem. Eng. J. 168 (2011) 1296-1300.
[3] L. Zhang, B. Sheng, Z. Xin, Q. Liu, S. Sun, Bioresource Technol. 101 (2010) 8144-8150.
[4] V.G. Deshmane, Y.G. Adewuyi, Fuel 107 (2013) 474-482.
[5] M. Gan, D. Pan, L. Ma, E. Yue, J. Hong, Chinese J. Chem. Eng. 17 (2009) 83-87.
[6] O. Ilgen, Fuel Process Technol. 95 (2012) 62-66.
[7] J.R. Oliveira Lima, Y.A. Ghani, R. B. Da Silva, F. M. Batista, R.A. Bini, L.C. Varanda, J.E. De Olivera, Appl. Catal. A 445 (2012) 76-82.
[8] E. Rashtizadeh, F. Farzaneh, J. Taiwan Inst. Chem. Eng. 44 (2013) 917-923.
[9] P.L. Boey, G.P. Maniam, S.A. Hamid, Chem. Eng. J. 168 (2011) 15-22.
[10] M.E. Borges, L. Díaz, Renew. Sust. Energ. Rev. 16 (2012) 2839-2849.
[11] F. Qiu, Y. Li, D. Yang, X. Li, P. Sun, Bioresource Technol. 102 (2011) 4150-4156.
[12] B. Yoosuk, P. Krasae, B. Puttasawat, P. Udomsap, N. Viriya Empikul, K. Faungnawakij, Chem. Eng. J. 162 (2010) 58-66.
[13] P.D. Patil, V. G. Gude, S. Deng, Ind. Eng. Chem. Res. 48 (2009)10850-10856.
[14] M. Di Serio, R. Tesser, L. Pengmei, E. Santacesaria, Energ. Fuel 22 (2008) 207-217.
[15] X. Deng, Z. Fang, Y.H. Liu, C.L. Yu, Energy 36 (2011) 777-784.
[16] L. Wen, Y. Wang, D. Lu, S. Hu, H. Han, Fuel 89 (2010) 2267-2271.
[17] S. Al Zuhair, F.W. Ling, L.S. Jun, Process Biochem. 42 (2007) 951-960.
[18] Y. Liu, H. Lu, W. Jiang, D. Li, S. Liu, B. Liang, Chinese J. Chem. Eng. 20 (2012) 740-746.

[19] D. Vujicic, D. Comic, A. Zarubica, R. Micic, G. Boskovic, Fuel 89 (2010) 2054-2061.
[20] A. Chouhan, A. Sarma, Renew. Sust. Energ. Rev. 15 (2011) 4378-4399.
[21] J.P. Evangelista, T. Chellappa, A.C. Coriolano, V.J. Fernandes, L.D. Souza, A.S. Araujo, Fuel Process Technol. 104 (2012) 90-95.
[22] X. Liu, X. Piao, Y. Wang, S. Zhu, Energ. Fuel 22 (2008)1313-1317.
[23] C.V. De Moura, A.G. De Castro, E.M. De Moura, J.R. Dos Santos, J.M. Moita Neto, Energ. Fuel 24 (2010) 6527-6532.
[24] Q. Shu, B. Yang, H. Yuan, S. Qing, G. Zhu, Catal. Commun. 8 (2007) 2159-2165.
[25] H. Wu, J. Zhang, Q. Wei, J. Zheng, J. Zhang, Fuel Process Technol. 109 (2013)13-18.
[26] S.S. Vieira, Z.M. Magriotis, N.A. Santos, A.A. Saczk, C.E. Hori, P.A. Arroyo, Bioresource Technol. 133 (2013) 248-255.
[27] A. Carrero, G. Vicente, R. Rodríguez, M. Linares, G.L. Del Peso, Catal. Today 167 (2011) 148-153.
[28] L.D. Borges, N.N. Moura, A.A. Costa, P.R. Braga, J.A. Dias, S.C. Dias, J.L. De Macedo, G.F. Ghesti, Appl. Catal. A 450 (2013) 114-119.
[29] R.I. Kusuma, J.P. Hadinoto, A. Ayucitra, F.E. Soetaredjo, S. Ismadji, Appl. Clay Sci. 74 (2013) 121-126.
[30] Y.Y. Wang, T.H. DaNg, B.H. Chen, D.J. Lee, Ind. Eng. Chem. Res. 51 (2012) 9959-9965.
[31] J.A. Botas, D.P. Serrano, A. García, R. Ramos, Appl. Catal. B Environ. 145 (2013) 205-215.
[32] N.N. Mahamuni, Y.G. Adewuyi, Energ. Fuel 23 (2009) 3773-3782.
[33] A. Birla, B. Singh, S.N. Upadhyay, Y.C. Sharma, Bioresource Technol. 106 (2012) 95-100.
[34] S. Jain, M.P. Sharma, Bioresource Technol. 101 (2010) 7701-7706.
[35] S. Jain, M.P. Sharma, S. Rajvanshi, Fuel Process Technol. 92 (2011) 32-38.
[36] A. Joelianingsih, H. Maeda, S. Hagiwara, H. Nabetani, Y. Sagara, T.H. Soerawidjaya, A.H. Tambunan, K. Abdullah, Renew. Energ. 33 (2008)1629-1636.
[37] C.S. Choi, J.W. Kim, C.J. Jeong, H. Kim, K.P. Yoo, J. Supercrit. Fluids 58 (2011) 365-370.
[38] P. Sivakumar, S. Sindhanaiselvan, N.N. Gandhi, S.S. Devi, S. Renganathan, Fuel 103 (2013) 693-698.
[39] O.S. Stamenković, Z.B. Todorović, Lazić ML, Veljković VB, Skala DU, Bioresource Technol. 99 (2008)1131-1140.
[40] V.B. Veljković, O.S. Stamenković, Z.B. Todorović, M.L. Lazić, D.U. Skala, Fuel 88 (2009) 1554-1562.
[41] A.V. Marjanović, O.S. Stamenković, Z.B. Todorović, M.L. Lazić, V.B. Veljković, Fuel 89 (2010) 665-671.
[42] I. Lukić, Ž. Kesić, S. Maksimović, M. Zdujić, H. Liu, J. Krstić, D. Skala, Fuel 113 (2013) 367-378.
[43] A.G. Santos, A.S. Araujo, V.P. Caldeira, V.J. Fernandes, L.D. Souza, A.K. Barros, Thermochim. Acta 506 (2010) 57-61.
[44] O.S. Stamenković, V.B. Veljković, Z.B. Todorović, M.L. Lazić, I.B. Banković, D.U. Skala, Bioresource Technol. 101 (2010) 4423-4430.
[45] H. Sun, Y. Ding, J. Duan, Q. Zhang, Z. Wang, H. Lou, X. Zheng, Bioresource Technol. 101 (2010) 953-958.
[46] K. Hayat, M.A. Gondal, M.M. Khaled, S. Ahmed, A.M. Shemsi, Appl. Catal A 393 (2011) 122-129.
[47] R.K. Verma, K. Kumar, S.B. Rai, Solid State Sci. 12 (2010) 1146-1151.
[48] R. Kaur, S. Singh, O.P. Pandey, Physica B 407 (2012) 4765-4769.
[49] E.P. Barrett, L.G. Joyner, P.P. Halenda, J. Am. Chem. Soc. 73 (1951) 373-380.